Cancer Nanotechnology

RESEARCH Open Access

# Multi-sensitive functionalized niosomal nanocarriers for controllable gene delivery in vitro and in vivo

Najmeh Alsadat Abtahi[1,2], Saba Salehi[1], Seyed Morteza Naghib[1*], Fatemeh Haghiralsadat[3], Mohammadmahdi Akbari Edgahi[1], Sadegh Ghorbanzadeh[4] and Wei Zhang[4*]

*Correspondence: Naghib@iust.ac.ir; wei.zhang@dlut.edu.cn

[1] Nanotechnology Department, School of Advanced Technologies, Iran University of Science and Technology, Tehran, Iran
[2] Biomaterials and Tissue Engineering Research Group, Department of Interdisciplinary Technologies, Breast Cancer Research Center, Motamed Cancer Institute, ACECR, Tehran, Iran
[3] Medical Nanotechnology and Tissue Engineering Research Center, Yazd Reproductive Sciences Institute, Shahid Sadoughi University of Medical Sciences, Yazd, Iran
[4] State Key Laboratory of Structure Analysis for Industrial Equipment, Department of Engineering Mechanics, Dalian University of Technology, Dalian, China

## Abstract

MicroRNAs, which can contribute to numerous cellular functions through post-transcriptional silencing, have become well-documented candidates for cancer treatment applications, particularly in chemo-resistant cancers. Herein, several formulations were examined to optimize the essential parameters, and the niosomal formulation consisting of cholesterol:tween-80:DOTAP:PEG with 9:69:15:7 ratio had the best physicochemical parameters including spherical shape, high entrapment efficiency, small diameter (81 ± 0.65 nm), and appropriate positive charge (23 ± 0.64 mV). Here, we aimed to design a system with increased delivery efficiency which was tested by the encapsulation of miR-34a within niosome NPs and assessed the nano-niosomal delivery of miR-34a as a tumor suppressor in MCF-7 human adenocarcinoma cells. The results showed that our novel niosome systems with non-ionic surfactants can successfully eliminate cancer cells by increasing the expression of p53 and reducing the expression of NF-κB. In comparison with the free dispersion of miR-34a, the lysis of a nano-sized delivery system demonstrated a better cytotoxicity effect against cancer cells. Similar results were obtained by performing in vivo test on the 4T1 xenografted Balb/C mouse tumor model and the miR-34a-loaded niosomes displayed a better reduction in tumor size by improving approximately + 13% in tumor inhabitation rate while maintaining the bodyweight close to the first day. Therefore, it is concluded that miR-34a delivery via niosomes has high potential as a tumor suppressor and a reliable procedure for breast cancer treatment.

**Keywords:** miR-34a, Niosome, Breast cancer, Tumor suppressor, Gene delivery, MCF-7

**Graphical Abstract**

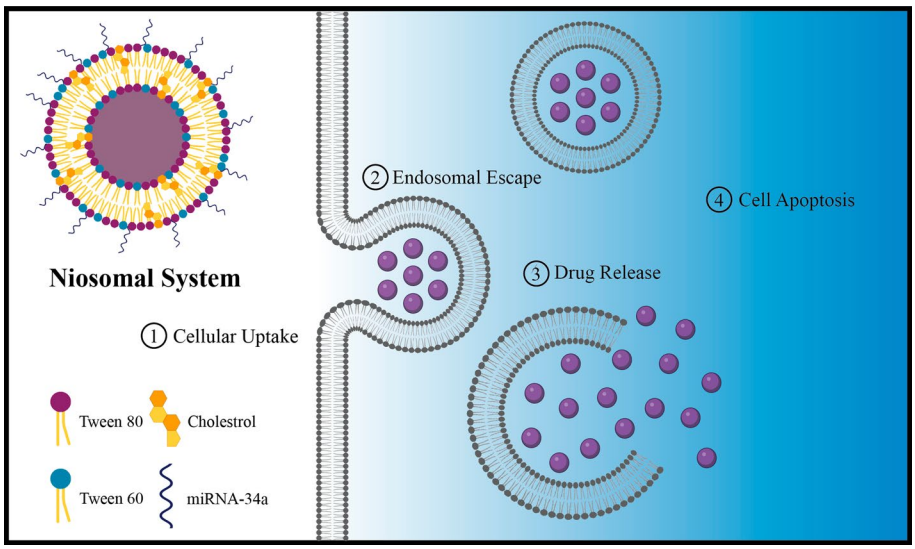


## Introduction

During the last few years, breast cancer has become one of the most common cancers in the world (Akhlaghi et al. 2022; Rahimzadeh et al. 2021; Sadeghi et al. 2022a; Sadeghi et al. 2022b; Yaghoubi et al. 2021). About 48 people in 100,000 were diagnosed with breast cancer in 2020 and it is one of the most prevalent cancers in the world (12.5% of all cancers diagnosed) (Smaili et al. 2020). While breast cancer-related deaths have decreased by nearly 40% in the last 40 years in high-income countries, it remains a huge burden of morbidity and mortality in low-income countries like Somalia or Syria (Siddiqui et al. 2021). Breast cancer can be induced by major issues like family history (genetics), hormonal risk factors, variation in lifestyle, and environmental changes (Francies et al. 2020). The exact etiology of breast cancer is not well defined and is most likely multifactorial, involving both genetic and environmental factors (Abtahi et al. 2021, 2022 ; Mazidi et al. 2022; Momenimovahed and Salehiniya 2019). Chemotherapy remains the main therapeutics for combating cancer. In the clinical treatment of breast cancer, the prescription of chemotherapy is always dependent on breast tumor pathophysiology and staging. Nonetheless, breast cancer resistance and relapse are growing issues and so are other disorders probability linked to chemotherapy due to the drug toxicity and non-targeted approaches (Alkabban and Ferguson 2018). Therefore, high toxicity on cancer cells with minimum impact on healthy cells must be guaranteed (Cheok 2012). To increase and improve clinical results, novel procedures have been developed, including hormone therapy, gene therapy, and combined therapy. MicroRNA-based anticancer therapies are being developed alone or in combination with current targeted therapies, to eliminate cancer cells and improve the success rate (Garzon et al. 2010).

In the initiation and development of cancer cells, several abnormalities in the modulation and expression of signaling pathways occur. Protein 53 (P53) is a tumor suppressor protein that induces responses at critical cellular stresses like DNA damage and oncogenes activation. It can also change the expression of several genes captured through increased DNA repair, apoptosis, regulated cell cycle, as well as prevention of angiogenesis. Mutations in the p53 gene are reported as the most common genetic change in human tumors and are often associated with increased proliferation and metastatic potential (Rahmani et al. 2019).

MicroRNAs (miRNAs) are a small size (~22 nucleotides single-stranded) category of conserved RNAs with non-coding ability that adjust gene expression at the post-transcriptional stage and they are vital in tumorigenesis. Several reports highlighted a significant reduction in specific microRNAs that have a tumor suppressor role within the adjacent tumor microenvironment. Of these microRNAs, a decrease in the level of families of 15a, 16–1, 143, 145, let-7, and 34 has been seen (Brannon-Peppas and Blanchette 2004; Schoof et al. 2012). Furthermore, a tumor suppressor miRNA family transcriptionally activated by p53 is microRNA-34 (miR-34), which has been implicated integrally as a component of the tumor suppressor pathway in cancer development (Navarro and Lieberman 2015). One of the most regular types of miRNAs that is induced by P53 is the miR-34 family which can control apoptosis and cell cycle of a variety of genes like CDk4 (cell cycle), Bcl-2 (apoptosis), and CD44 (metastasis). MiR-34a, a member of this family, is commonly found dysregulated in some tumors, including breast tumors which may be linked to the stemness of some of the breast cancers (Agostini and Knight 2014). MiR-34 stands out as a critical mediator. Numerous reports have confirmed that the expression of miR-34a can prevent proliferation, migration, invasion, metastasis, and the epithelial-to-mesenchymal transition of cancer cells (Bader et al. 2010) (Jemal et al. 2011).

Recently, vesicular drug delivery systems have attracted significant attention for their remarkable properties, such as a reduction of side effects, high encapsulation efficiency, prolonged blood circulation, and increased drug solubility. For microRNA delivery applications, niosomes and liposomes are two suitable vesicles (Bader et al. 2010; Brannon-Peppas and Blanchette 2004; Schoof et al. 2012). Niosomes are structurally unilateral or multilateral with the ability to carry hydrophobic and hydrophilic genes, therapeutic agents, or drugs. They can be categorized as cationic, non-ionic, anionic, and amphoteric surfactant-based vesicles according to their head regions that are biodegradable, stable and low cost, easy to formulate and scale up, and practically non-toxic. (Bartel 2004). Because of their forming materials (non-ionic surfactants), with or without cholesterol, they are more stable physically and chemically than those of lipids like the ones that compose liposomes (Bartelds et al. 2018). Thus, over the years and with novel approaches being reported, niosomes have become an excellent and inexpensive alternative for drug delivery (Bartelds et al. 2018).

In this experiment, novel microRNA-based treatments have been explored regarding appropriate cellular uptake and toxicity in both in vitro and in vivo conditions. Herein, we synthesized niosomal systems in various compositions of materials to investigate and find the optimum formulation according to the physicochemical properties. The optimum formulation was selected and miR-34a in various concentrations was loaded within the nanocarriers. The miR-34a-loaded niosomes were subjected to MCF-7 breast

adenocarcinoma cells and 4T1 xenografted Balb/C mouse tumor to evaluate the antitumoral efficacy for in vitro and in vivo studies, respectively. Eventually, the results were measured and presented as mean ± SD to find the best state of cancer treatment method.

## Materials and methods

### Materials

For the experiment, human breast cancer cells (MCF-7, Pasteur Institute, Tehran), microRNA-34a (Zist Avaran, Iran, Tehran), PEG (Lipoid GmbH, DSPE-mPEG 2000, Lipoid PE 18:0/18:0-PEG2000, Darmstadt, Germany), DAPI (40, 6- diamidino-2-phenylindole, Thermo Fisher Scientific, MA, USA), Tween-80 (DaeJung Chemicals & Metals Company, Seoul, Korea), cholesterol, PBS (phosphate-buffered saline) tablets, DOTAP (1,2-dioleoyl- 3-trimethylammonium-propane), paraformaldehyde solution, MTT 3-(4, 5-dimethylthiazol-2-yl)-2, Sigma-Aldrich, MO, USA) were acquired. No further purification was applied for the salts, solvents, or any other chemicals with analytical grades, except those mentioned.

### Niosome preparation

To formulate niosomes, the thin-film hydration technique was utilized. The calculation of Tween-80 and cholesterol was precisely done and then dispersed in 100 mL of chloroform C. With a rotary flash evaporator (Ultrasonics GmbH, Heidolph, Germany) and at a decreased pressure, a lipid film was shaped. After that, with 3 mL of PBS at pH 7.4 and 60 °C, the lipid film was hydrated. For decreasing the average size of vesicles, a microtip probe sonicator was utilized for 30 min to sonicate the hydrated film. The physical characteristics of all formulations were monitored. In the next step, the stability of niosomal formulations was enhanced by inserting cationic lipid DOTAP and PEG. With the use of a rotary evaporator, the solvent was fully dried at 45 °C. In a similar way, the layers were hydrated via the addition of PBS for 45 min to obtain niosomal suspension and sonicated to reduce the average size of vesicles.

### Physical characterization

With the help of ZetaPALS particle size (Holtsville, Brookhaven Instruments, NY, USA), zeta potential (ZP) analyzer, and dynamic light scattering (DLS), characteristics including the size of niosome particles, polydispersity index (PDI), and ZP were evaluated. Also, AFM (model AFM5100N, HITACHI), SEM, and TEM were obtained to assess the morphology of nanocarriers.

### Physical stability examination

For the determination of the physical stability of niosomes, the test lasted 90 days. Variations in the size of the particle and differences in ZP and PDI were assessed on the 30th, 60th, and 90th days (Asthana et al. 2016; Ceren Ertekin et al. 2015).

### Cell lines and culture conditions

Cell culture condition was applied to human breast cancer cells, MCF-7, which was acquired from the Iranian Biological Resource Center (Tehran, Iran). Also, a mixture of Ham RPMI1640 (InoClon, Tehran, Iran), augmented with 15% of FBS, 2 mM

GlutaMAX™-I (100X), and 1 mg/mL$^{-}$ penicillin/streptomycin, and Ham DMEM/F12 (InoClon, Tehran, Iran), augmented with 5% horse serum (Gibco, MA, USA), 100 ng/mL cholera toxin, 0.5 µg/mL hydrocortisone, 2 mM GlutaMAX™-I, EGF 20 ng/mL, 10 µg/mL insulin (Sigma-Aldrich, MO, USA), and 1 mg/mL penicillin/streptomycin was prepared.

#### Cytotoxicity examinations

With the help of MTT assays, the cytotoxicity of various concentrations was investigated. All cell lines were seeded in 96-well plates at $10^4$ cells/well concentration. First, the attachment process was applied for one day. Afterward, 200 µL of new medium was added to cells, consisting of various dilutions of the niosomal miR-34a formulations comprising free niosome, niosomal miR-34a, and free miR-34a solution. Next, samples were incubated for the following 1, 2, and 3 days, then, in every 96-well plate, 20 µL or 5 mg/mL of MTT in PBS was inserted. Next, the drug-containing samples were incubated for 3 h at 37 and 42 °C. For dissolving the shaped formazan crystals, 180 µL of dimethyl sulfoxide was inserted into the wells and the medium was cautiously removed. For recording the absorption rate, each plate was assessed using an EPOCH Microplate Spectrophotometer (570 nm, synergy HTX, BioTek, VT, USA). The cytotoxicity data were reported as the Inhibitory Concentration ($IC_{50}$) value, which represents the minimum concentration of therapeutic agent to restrict the proliferation of 50% of cells compared to the control group (Balakrishnan et al. 2009; Wang et al. 2016).

#### Nanoniosomal cellular uptake

In this assessment, all cell lines were seeded in 6-well plates at $2 \times 10^5$ concentration. Next, to achieve desired attachment, an incubation process was applied for one day. Afterward, for cell treating purposes, free miR-34a, niosomal miR-34a, and free niosome were utilized. After 3 h of the incubation step, the rinsing process was accomplished with low-temperature PBS 3 times and then they were fixed with paraformaldehyde (4%). In addition, for photography applications, a fluorescence microscope (BX61, Olympus, Japan) and for cell marking purposes DAPI (0.125 µg/mL, Thermo Fisher Scientific, MA, USA) were utilized. MiR-34a was conjugated to fluorescein amidites (FAM), which emits a red-colored fluorescence signal (Alemi et al. 2018; Lin et al. 2012; Lv et al. 2014).

#### Apoptosis assay

In this research, the Annexin V- FITC/PI double staining procedure was performed. To calculate the apoptosis rate, MCF-7 cells were seeded in a 6-well plate at $10^5$ cells/well concentration. Here, cells were subjected to the free miR-34a and different formulations at the $IC_{50}$ concentration for all the drugs. After incubation for 1 day, to detach the cells, 0.25% trypsin/EDTA was used, and then, it was centrifuged for 3 min at 1500 rpm. Next, 3 µL of Annexin V-FITC solution was added to the suspension of the pellet and ice-cold PBS at pH 7.4. Moreover, to identify the necrotic cells, 3 µL of propidium iodide (PI) was also added to the suspension. Ultimately, the suspension was incubated for 30 min on ice and analyzed by flow cytometry (BD FACSCalibur instrument), respectively.

### In-vivo Experiments

To perform *in-vivo* examination according to NIH and IACUC guidelines, 35 6- to 8-week female BALB/c mice (Pasteur Institute, Tehran, Iran) with 20 to 25 g bodyweight were purchased and kept in a sterilized condition. First, each mouse was treated with $5 \times 10^6$ 4T1 cells subcutaneously into the right flank. Next, they were randomly divided into 4 groups of 5 mice when the tumor reaches 100 $mm^3$. Free miRNA with 2.5 mg/kg and niosomal miRNA (B) with 10 µg per mouse were injected within the tail vein of each group of mice. For the control group, normal saline was injected. The injections were repeated every 3 days up until 12 days and at each interval, the tumor size and bodyweight of each mouse were measured. All mice were killed on the 21st day. The tumor size was measured according to the equation:

$$\mathrm{V}\left(mm^3\right) = \frac{LW^2}{2}$$

where V represents the volume of the tumor, L and W are the lengths of the tumors, respectively. Also, the equation below was utilized to measure the inhibition rate (Alsadat et al. 2022):

$$\text{Tumor inhibition rate}(\,TIR, \%) = \frac{W_c - W_t}{W_c} \times 100$$

where $W_c$ and $W_t$ represent the average weight of tumors in the control and treated groups, respectively.

### Statistical analysis

Recording, editing, and entering the obtained data were done via GraphPad Prism software v6.00 (San Diego California USA). All the data were at least triplicates and presented as average ± SD. To evaluate separate categories, ANOVA tests were utilized. P-values lower than 0.05 were stated as significant.

## Results

### Physicochemical characterization of complexes

By assessing the synthesized complexes, the formulations were listed according to their size, ZP, and PDI (Tables 1 and 2). In the nanocomplexes preparation process, Tween-80 was utilized as the base surfactant, and by increasing the level of cholesterol, several changes, especially in the average size of niosome diameter, were

**Table 1** The physicochemical influence of cholesterol and Tween-80 composition at various molar ratios on ZP, PDI, and vesicle size

| Code | Cholesterol (%) | Tween-80 (%) | ZP (mV) | PDI | Size (nm) |
|---|---|---|---|---|---|
| F1 | 5 | 95 | − 23 ± 0.08 | 0.234 ± 0.65 | 122 ± 0.39 |
| F2 | 15 | 85 | − 21 ± 0.37 | 0.265 ± 0.76 | 115 ± 0.67 |
| F3 | 25 | 75 | − 24 ± 0.76 | 0.264 ± 0.55 | 123 ± 0.56 |
| F4 | 35 | 65 | − 22 ± 0.32 | 0.215 ± 0.63 | 125 ± 0.45 |
| F5 | 45 | 55 | − 22 ± 0.49 | 0.263 ± 0.18 | 117 ± 0.65 |

**Table 2** The physicochemical effects of the addition of PEG and DOTAP in F2 composition at various molar ratios on ZP, PDI, and vesicle size

| Code | Cholesterol (%) | Tween-80 (%) | DOTAP (%) | PEG (%) | ZP (mV) | PDI | Size (nm) |
|---|---|---|---|---|---|---|---|
| F6 | 13 | 80 | – | 7 | − 19 ± 0.15 | 0.209 ± 0.35 | 109 ± 0.11 |
| F7 | 11 | 77 | 5 | 7 | 1 ± 0.98 | 0.186 ± 0.42 | 99 ± 0.87 |
| F8 | 10 | 73 | 10 | 7 | 12 ± 0.54 | 0.174 ± 0.87 | 88 ± 0.56 |
| F9 | 9 | 69 | 15 | 7 | 23 ± 0.64 | 0.150 ± 0.23 | 81 ± 0.65 |

observed (F1 → F5, Table 1). However, the surfactant cholesterol ratio had no significant effect on the vesicle ZP and PDI. Also, PDI < 0.3 demonstrates no aggregation in vesicles. Ultimately, the F2 formulation was selected for further investigation. In the next assessments, samples were prepared by putting them on a carbon-covered copper screen and then uranyl acetate was added. After waiting for 2 min to dry, they were rinsed with distilled water and exposed to 100 kV. PDI, ZP, vesicle size, and physical stability of all formulations were evaluated by storing them at 4 °C for 90 days.

To obtain further stability, the F2 was selected and the effect of PEG and DOPAT on its physicochemical parameters was evaluated. The next formulations (F6 → F8) exhibited lower PDI and smaller diameter sizes than their reference (Table 2). Technically, favorable interaction of nucleic acid with negative charge happens when the delivery system is positively charged. Therefore, through the addition of 5, 10, and 15% of DOTAP, a modification in the charge of the particles was observed. In F9, a remarkable enhancement in the charge was detected. The findings showed that the F9 including Tween-80; cholesterol:PEG:DOTAP with the molar ratio of 1.6:0.2:0.4:0.17 had the best characteristics.

Herein, a new niosomal PEGylated cationic formulation for miR-34a transfer was improved. The synthesized NPs made of Tween-80 as a reliable surfactant and cholesterol as a stabilizer factor, increased the niosome mean diameter (Matsumura and Maeda 1986). Adding PEG resulted in the reduction and promotion in mean size diameter and stability, respectively (Li et al. 2014). With the addition of 7% PEG to the F5, the resulting formulation (F6) demonstrated a smaller PDI and diameter. Furthermore, vesicle size, PDI, and transfection effectiveness were influenced by the presence of cationic lipids (DOTAP). As mentioned before, by adding 5–15% cationic lipids (F7-F9), a reduction in vesicle size and PDI and growth in ZP was observed. To facilitate vesicle interruption and aggregation, it is critical for charge introduction on surfaces. An appropriate indicator of this barrier size is ZP. When the ZP is high, particles can strongly repel each other and subsequently have minimum aggregation (Matsumura and Maeda 1986). After 3 months of storage, having DOTAP and PEG in the complexes demonstrated constant behavior and there was a similarity between all other physical properties. Also, TEM, SEM, and AFM were utilized to assess the structure of the niosome. Figure 1 presents the morphology of F9 which was spherical and in vesicular form (Fig. 1e, f) that had round structures with smooth surfaces.

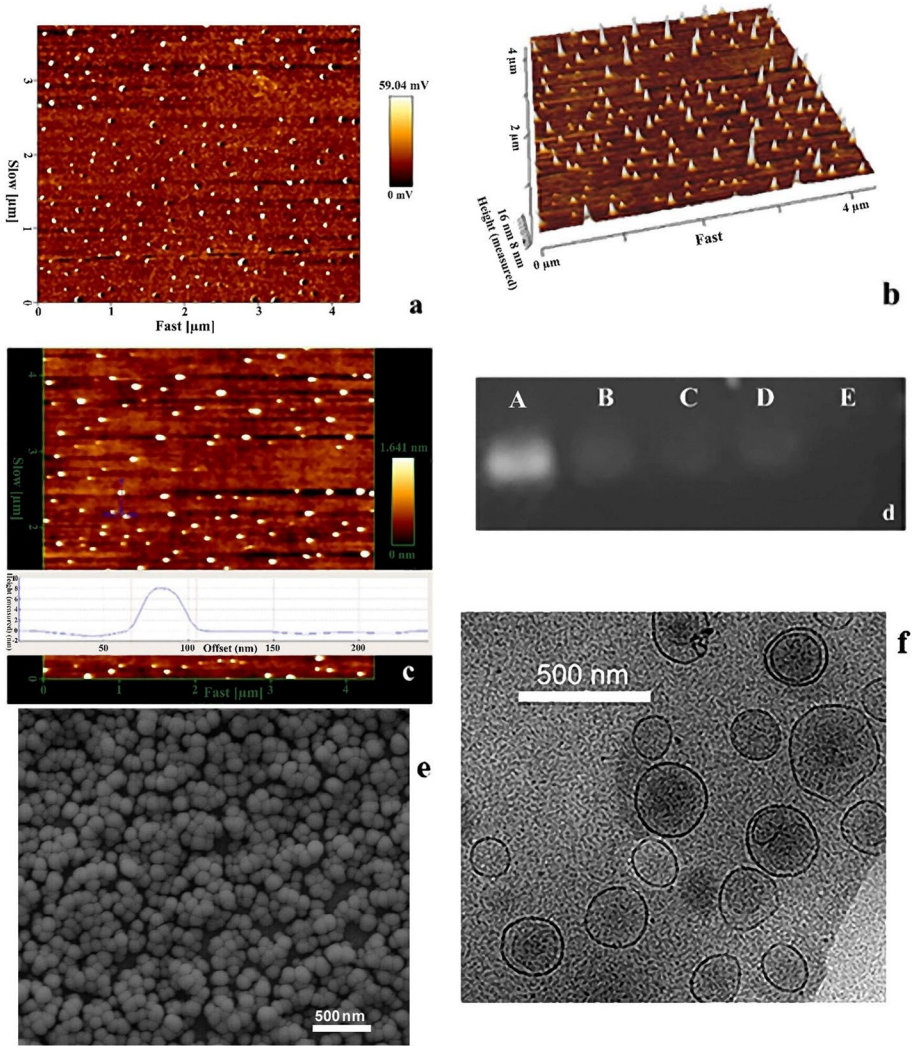


**Fig. 1** AFM imaging of nanocomplex in **a** 2D, **b** 3D, and **c** line analysis forms. **d** Formation of miR-34a-loaded cationic niosome. **e** SEM and **f** TEM imaging of miR-34a-loaded cationic niosome

**Table 3** The physicochemical features of nanoparticles with miR-34a

| Code | miR-34a (ng) | PDI | Size (nm) | ZP (mV) |
|---|---|---|---|---|
| **A** | none | 0.125 ± 0.81 | 120 ± 0.45 | 4 ± 0.87 |
| B | 1 | 0.124 ± 0.04 | 117 ± 0.16 | 8 ± 0.45 |
| C | 0.5 | 0.123 ± 0.86 | 113 ± 0.54 | 11 ± 0.87 |
| D | 0.25 | 0.120 ± 0.53 | 111 ± 0.09 | 12 ± 0.54 |
| E | 0.125 | 0.118 ± 0.12 | 100 ± 0.65 | 15 ± 0.18 |

### Encapsulation of miR-34a

In this context, a novel illustration of the evaluated nanocomplex is needed to estimate the effect of macromolecules on the physicochemical characteristics of the nanosized carrier. To measure the average size, PDI, and ZP of free and miR-34a-loaded NPs,

DLS analysis was utilized. First, the incubation process of various volumes of miR-34a in nanoplexes (F9) was done and followed by an incubation process at 37 °C for 60 min. With the use of TAE buffer gel electrophoresis was accomplished on agarose gel (1% (w/v)) at 120 v for 40 min (Fig. 1d). The results are listed in Table 3 as A, B, C, D, and E representing free, 1, 0.5, 0.25, and 0.125 ng miRNA, respectively.

### Leakage stability

To investigate the effect of prolonged storage of microRNA on leakage from nanoplexes, the complexes were reserved at 4 °C for 90 days. As shown in Fig. 2a for the entire organized formulation, the stability was assessed through a spectrophotometrical measurement at 260 nm. The results demonstrated that all of the complexes maintained their stability at the end of the 90th day; B and E obtained the highest and lowest leakage, respectively.

### Zeta potential stability and size

According to Fig. 2b, c, the size and ZP of every microRNA nanoplexes formulation were observed in 90 days. It was revealed that code B owned the most variation in diameter and code E exhibited the most stable formulations. Nearly, the same results recurred in ZP, by which the size trend reduced and ZP increased.

### Cytotoxicity assays

Nanoplexes that have been loaded with miR-34a were evaluated in their in vitro antitumor effect which was accomplished with MTT assay on MCF-7 as the cancerous cells and the results presented in Fig. 3 as $IC_{50}$ values, in pH 6.5 and 7.4 after 24, 48, and 72 h. According to the results, it was found that at pH 7.4 and lower temperatures, cells required higher concentrations of either free miRNA or niosomal miRNA

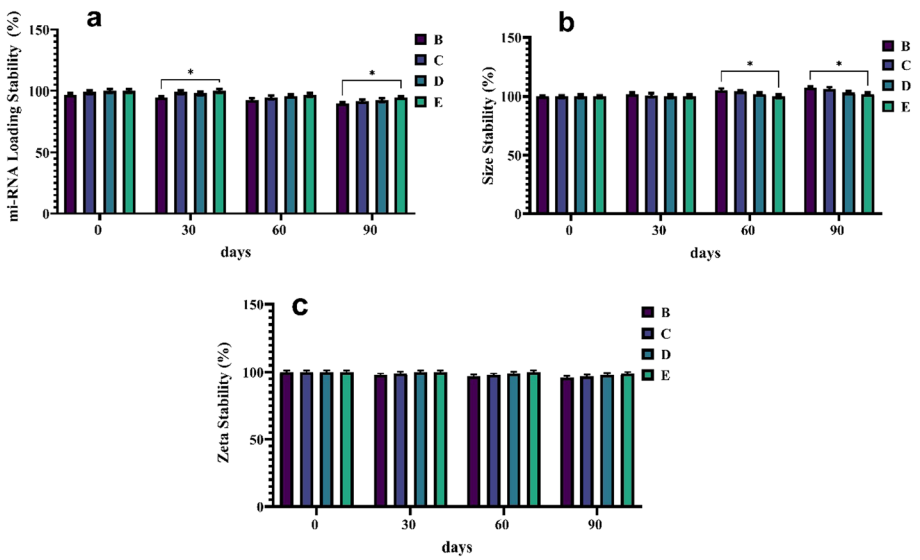


**Fig. 2** **a** Time-dependent stability of miR-34a-loaded niosomes. **b** and **c** Size and zeta potential stability of mi-RNA 34a niosomes after 0, 30, 60, and 90 days

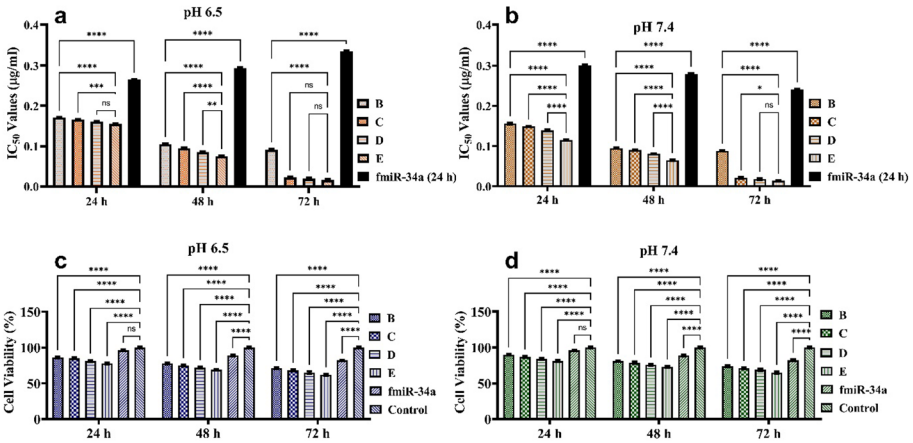


**Fig. 3** $IC_{50}$ values of various formulations of miR-34a niosomes at pH **a** 6.5 and **b** 7.4. Cytotoxicity of unloaded niosome and various formulations of miR-34a niosomes on cancer cells with MTT assay during 24, 48, and 72 h at pH **c** 6.5 and **d** 7.4

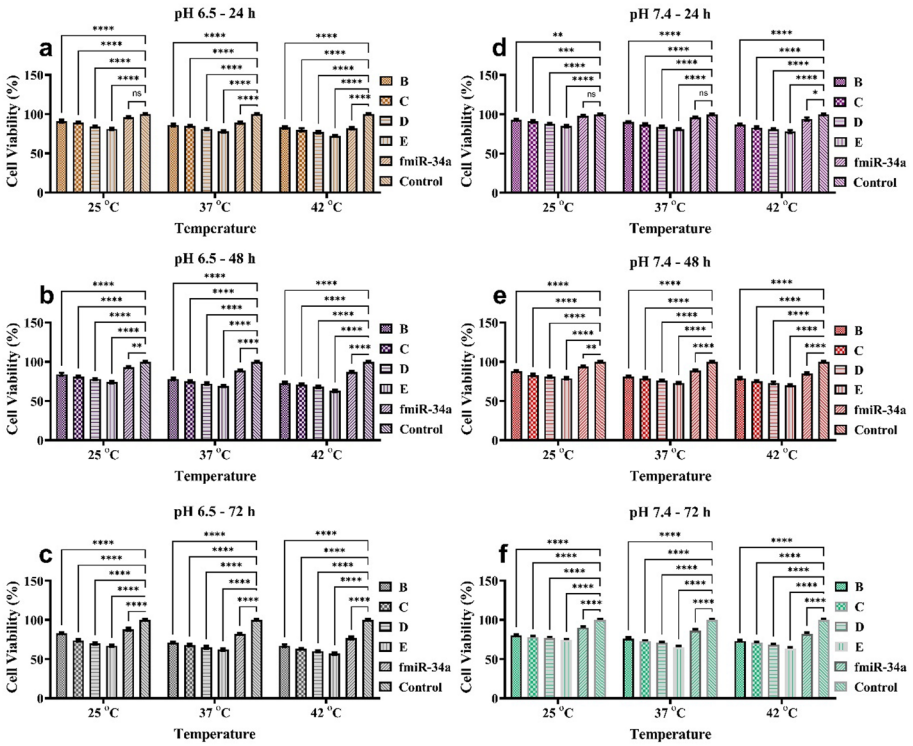


**Fig. 4** **a**, **b**, and **c** Cytotoxicity of unloaded niosome and various formulations of miR-34a niosomes on cancer cells with MTT assay at 25, 37, and 42 °C during 24, 48, and 72 h at pH 6.5. **d**, **e**, and **f** Cytotoxicity of unloaded niosome and various formulations of miR-34a niosomes on cancer cells with MTT assay at 25, 37, and 42 °C during 24, 48, and 72 h at pH 7.4

to reach $IC_{50}$ than at higher temperatures and more acidic pH. In addition, the use of a nanocarrier reduced the $IC_{50}$ compared to free miRNA and after 72 h of incubation, the gap in $IC_{50}$ values between the niosomal and free forms enlarged significantly.

As shown in Fig. 4, by adding miR-34a-loaded nanoplexes to the cells, it was observed that cell viability significantly reduced gradually after 2 days. Similarly, the impact of free miR-34a or niosome on the MCF-7 cell line was investigated. The level of cancer cells decreased at various concentrations of miR-34a. Ultimately, code E had the highest influence on cancer cells than the other codes (Fig. 4). Also, by increasing temperature and decreasing pH, the cytotoxicity of the drug on cells increased.

#### MiR-34a niosomal cellular uptake tests

The investigations were accomplished to evaluate the cellular uptake efficiency of miR-34a niosomal formulation, which was done on MCF-7 cell modeling the cancerous cells. Niosome nanovesicles via endosomal trafficking can merge with the cell membrane and intracellularly deliver miRNA. The adsorption of miR-34a was

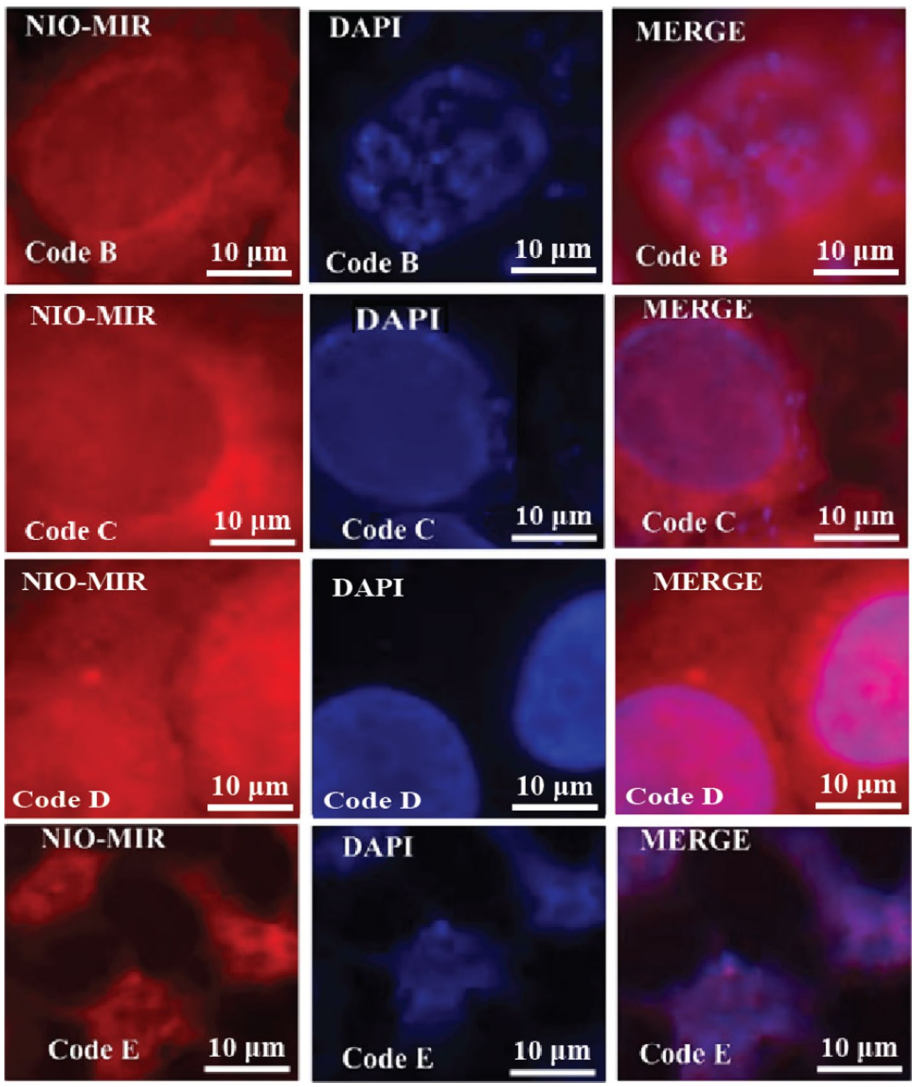


**Fig. 5** Cellular uptake images of cancer cells incubated with various formulations of miR-34a physical mixture for 4 h

observed via marking the stimulation of miR-34a using FAM fluorescent dye to monitor the cell uptake behavior. As shown in Fig. 5, after the incubation process for 4 h, miR-34a which was marked with FAM, was visible in the perinuclear region of the cytoplasm (market spots seen as red). The presence of miR-34a inside the cell cytoplasm was more obvious via the utilization of niosomal carriers than in the free forms in all cell lines and code E had the highest penetration. Technically, endocytosis has a notable influence on the penetration of niosomes inside the cells through cells' membranes by a diffusion mechanism (Bader et al. 2011; Fernandez-Piñeiro et al. 2017; Matsumura and Maeda 1986; Okada et al. 2014).

### Apoptosis analysis

The annexin V-FITC/PI double staining assay was performed to evaluate the toxicity of samples within 24 h and the quantitative data was analyzed using a flow cytometer. Technically, by the inward to the outward translocation of the membrane's phospholipid phosphatidylserine (PS), and exposing the PS to the exterior cellular environment, cell death can be detected. Annexin V is a calcium-dependent phospholipid-binding protein that has a high affinity to bind with PS that existed in the cellular environment. Moreover, annexin V is able to conjugate fluorescent molecules such as fluorescein isothiocyanate (FITC) while maintaining its affinity. In addition, to stain DNA, propidium iodide (PI) was used. The reason was that PI is not capable of penetration in live or early apoptotic cells. Therefore, it can only stain the DNA of dead cells which can be exploited to separate the live cells, early apoptotic cells, late apoptotic cells, and necrotic cells. Ultimately, the detection of conjugated annexin V-FITC and PI can be a suitable parameter to measure the apoptosis rate by a sensitive probe of flow cytometry. Based on the scatter plot of the double-variable flow cytometry, Q1, Q2, Q3, and Q4 quadrants (FITC + /PI −) demonstrate the necrotic, late apoptotic, early apoptotic, and living cells, respectively. Cells subjected to code E had the highest apoptosis rate than any other formulation (Fig. 6).

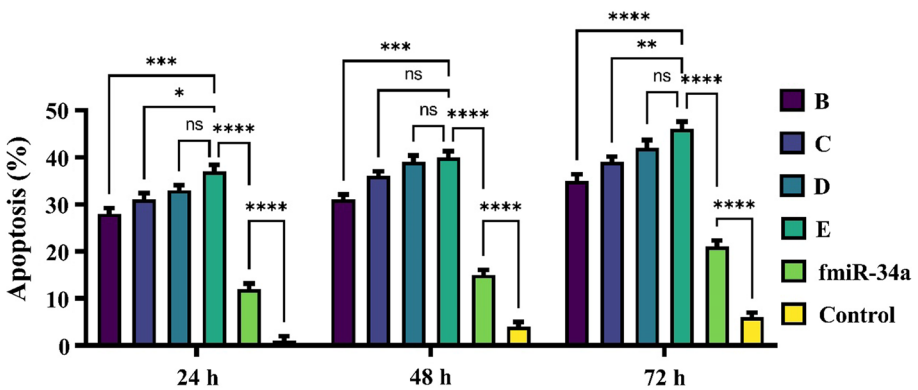


**Fig. 6** The apoptosis rate of cells subjected to the various formulations, free miR-34a, and none as the control group after 24, 48, and 72 h

### Gene expression

In this experiment, the gene silencing efficiency of miR-34a was examined by measuring the expression of p53 and nuclear factor-kappaB (NF-κB) using qRT-PCR techniques. Generally, the expression of the Nf-κB gene is connected to the growth of cells and reducing its expression influences the proliferation of normal and cancer cells. Nf-κB induces cell death via mitochondrial apoptosis pathways and a higher level of Nf-κB can considerably affect the viability of normal cells. Hence, controlling the expression of p53 and Nf-κB genes is vital for medicine. After subjecting cells to the samples, slight changes in the expression of p53 and Nf-κB were detected. Free miR-34a increases the level of p53 but decreases the level of NF-κB gene expression compared to the control group (Fig. 7a and b). However, the utilization of niosomal carriers considerably enhanced the expression of both p53 and Nf-κB genes, compared to the free form. Code E demonstrated the highest effectiveness in the reduction of the NF-κB and expression of p53 than any form alone.

### In-vivo tumor inhibition

To assess the antitumor activity of formulation E, 4T1 xenografted Balb/C mouse tumor models were conducted. The mice from each group were subjected to one medicine including free miR-34a and niosomal miRNA (E), as well as normal saline, every 3 days until 12 days. Medicines were injected into the tail vein of the mice. After 21 days, to evaluate the tumor volumes after the killing and removal, a digital vernier caliper was employed. The results demonstrated that free miR-34a groups displayed a reduction in

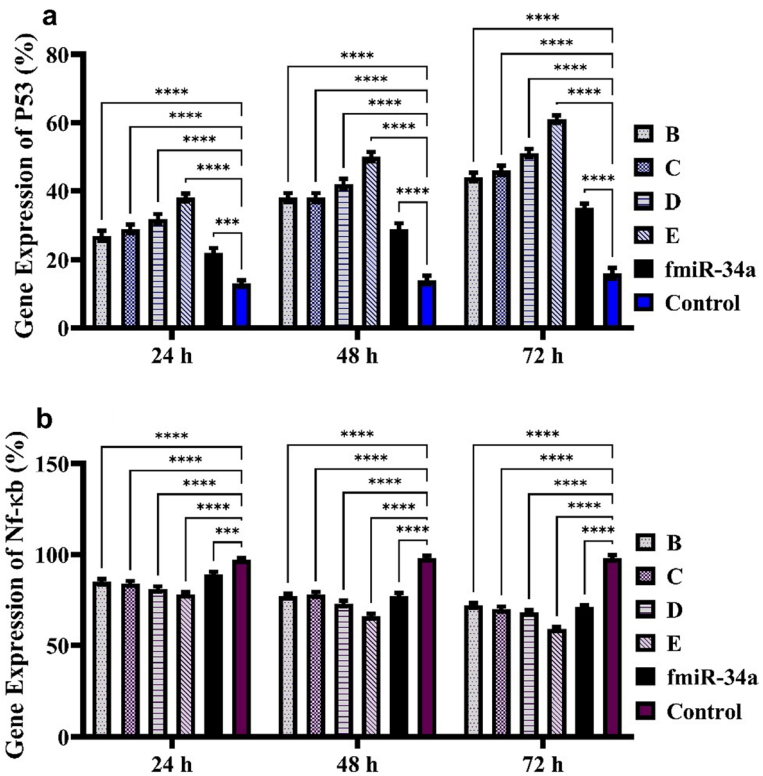


**Fig. 7** qRT-PCR analysis of the expression of **a** p53 and **b** Nf-κB of the same samples after 24, 48, and 72 h

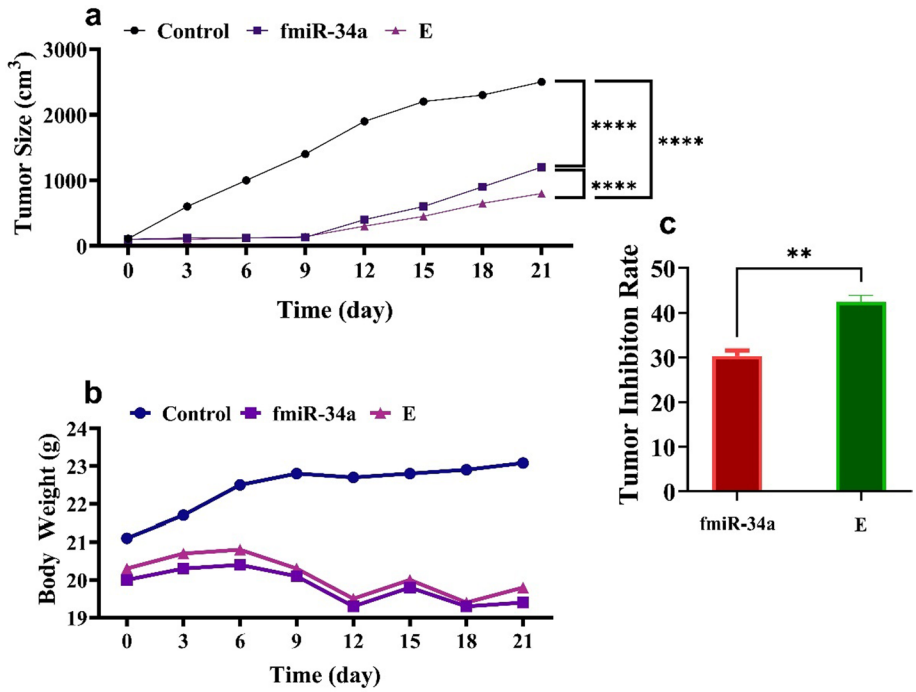


**Fig. 8** The effects of different medicines on mice groups after 21 days at every 3-day intervals on **a** tumor size, **b** bodyweight, and **c** the ultimate tumor inhibition rate

the tumor size compared to the saline group. Likewise, the niosomal miR-34a (E) group had even smaller tumors than the other groups (Fig. 8). It can be concluded that the decrease in cell growth was the result of the constant inhibition by the samples. The data concluded that niosomal miR-34a could enhance the tumor inhibition activities and also it presented an augmented therapeutic impact on cells more than that of free miR-34a (Fig. 8). The cytotoxicity of all medicine was assessed by weighing the mice at each interval (Fig. 8). The bodyweight of treated mice encountered a minor reduction after 21 days, whereas the saline group gained weight.

## Discussion

MicroRNAs are capable of regulating the level of expressing genes; therefore, they have turned into an effective method for cancer therapy and can adjust pathways that have an essential role in the progress of tumor growth. Besides, unique microRNA expression characteristics are related to special cancer forms. Therefore, by exposing such microRNA in the tumor area, they show a down-regulated activity which can be exploited as an alternative treatment with tumor-suppressing characteristics. Since the purpose of this method is to mimic microRNA activity, its release into an RNA-induced silencing complex (RISC) is needed, resulting in the silence of its target microRNAs. In comparison with single-stranded microRNA mimics which are used for RISC loading purposes, double-stranded is more efficient owing to suitable structures to make RISC loading easier and improve gene silencing effectiveness. Delivering microRNAs to cancerous tissues is the most important challenge to overcome because they can easily and rapidly degrade by a nucleus. The time duration between injection and adsorption of microRNA

is crucial to minimize the degradation and maximize the effectiveness. In addition, negative charge and molecular weight hinder the entrance of the mimicking microRNA into the cell. To overcome such problems, nanocarriers are highly recommended. Nanotechnology is an effective method to enhance the delivery efficacy of therapeutic molecules to the tumor site. In nanotechnology, different materials such as colloidal formulation and polymeric materials are highly developed and used in clinical therapy. The novel pharmaceutical method for old drug encapsulation has led to efficient drug delivery systems with a lower quantity of drugs and consequently lower side effects (Barani et al. 2019b; Barani et al. 2019a).

Our study demonstrated that the delivery of miR-34a by the nanoniosome to the cell increased the expression of the p53 protein. The investigation for miR-34a transfer applications has developed a novel PEGylated niosomal formulation. The nanoparticles were made of Tween-80 as the surface surfactant and the comparison in size, PDI, and ZP of various formulations was accomplished. In fact, cholesterol plays a stabilizer role and by increasing cholesterol content, niosomes' mean diameter increases. The existence of PEGylation in niosome formulation resulted in improved stability and reduction in the mean size diameter. Therefore, 7% niosome polyethylene glycol was added to F5. In comparison with F5, the F6 formulation owns a smaller PDI and diameter. Also, transfection efficiency, PDI, and vesicle size were influenced by DOTAP (cationic lipids) presence. By adding 5–15% DOTAP to the F6 formulation, ZP enhanced and a reduction in the mean size and PDI was observable. In addition, to prevent vesicular aggregation, applying a charge to their surface was a suitable approach. Next, by the storage of the samples for 2 months, the presence of PEG and DOTAP in the system was confirmed and also had similar physical properties.

The effect of free miR-34a or niosome on the MCF-7 cell line was investigated. The level of the cancer cells faced a significant decrease in various concentrations of miR-34a. The cellular uptake tests were conducted by the exposure of free miR-34a, free niosome, and miR-34a-loaded niosome to cells. The entrance of miR-34a into the cytoplasm was sharper with niosome than the free form of miR-34a on all cell lines. The efficiency of miR-34a on growth inhibition was also compared to miR-126 lipofectamine-treated MCF-7 cancer cells and the results showed that miR-34a in free and encapsulated forms induced higher cytotoxicity on the same cancer cells (Alhasan 2019; Davarpanah et al. 2018). The expression of p53 and NF-κB genes is directly connected to cell apoptosis and cell growth signaling pathways, by which a higher level of the p53 gene increases apoptosis rate and a lower level of NF-κB genes inhibits cell growth. Expression of the genes was investigated by niosome formulations, the assessments showed that p53 expression was considerably higher with the miR-34a-loaded niosome ($p < 0.05$), and the expression of the NF-κB gene was decreased using all formulations. As expected, the apoptosis of cancer cells was notably higher in miR-34a-loaded niosome than that of free forms.

The same outcome was obtained by performing in vivo test on 4T1 xenografted Balb/C mouse tumor models. In this study, after the tumor size reached the appropriate size, free miR-34a and niosomal miRNA (E), as well as normal saline were injected into each group every 3 days until 12 days. After 21 days, the result showed similar activity as in vitro study. The mice treated with miR-34a-loaded niosome could significantly diminish the tumor size while the bodyweight of mice faces a negligible

reduction compared to the free forms. Moreover, by measuring the tumor inhibition rate, it was concluded that the encapsulation of miR-34a in the niosomal delivery system promotes antitumoral activity while it had the minimum side effects on healthy cells.

## Conclusion

In cancer treatment, microRNAs are widely utilized since they are capable of deregulating gene expression in cancer tissues. This method of treatment is derived from the capability of microRNAs in expressing genes like p53 and adjusting pathways which play an important role in tumor progress and growth. In addition, there is unique microRNA expression for each particular form of cancer. The concept of microRNA treatment is based on down-regulating microRNAs, which results in recovering their level and tumor-suppressing property with substitute treatment with microRNA simulators. There is a requirement for loading microRNA simulators on an RNA-induced silencing complex to silence microRNAs. Among single-stranded and double-stranded microRNA simulations, double-stranded is more favorable, since it improves gene silencing effectiveness and makes RISC loading easier. One important concern related to microRNA cancer treatment is their delivery to cancerous tissues because they can easily and promptly degrade and clear via nucleases. In addition, negative charge and molecular weight hinder the entrance of microRNA mimics into the cell. Nano-sized carriers are an appropriate choice to solve these challenges. In this experiment, our group has progressed to a novel nanocarrier to enhance microRNA delivery to the site of the tumor. The investigation represents a stable formulation, sustained-release behavior, diameter of 115 nm, and high effectiveness of microRNA loading (with no destructive chemical reactions). Niosomes which have been loaded with microRNA represented robust cytotoxic impacts against MCF-7 and 4T1 xenografted Balb/C mouse tumor models, which confirms their potential as a promising way for breast cancer treatment.

**Abbreviations**

| | |
|---|---|
| NPs | Nanoparticles |
| PDI | Polydispersity Index |
| MTT | 3-(4,5-Dimethylthiazol-2-yl) |
| PBS | Phosphate-buffered saline |
| AFM | Atomic force microscopy |
| DAPI | 4′, 6-Diamidino-2-Phenylindole |
| PEG | Polyethylene Glycol |
| SEM | Scanning electron microscope |
| miR-34 | MicroRNA-34 |
| NF-κB | Nuclear Factor-kappaB |
| FBS | Fetal Bovine Serum |
| EGF | Epithelial (or epidermal) growth factor |
| RISC | RNA-Induced silencing complex |
| PLGA | Poly(lactic-co-glycolic acid) |

**Acknowledgements**
Not applicable.

**Author contributions**
NAA, SS and SMN convinced the idea and wrote and revised the manuscript. FH supported the research and provided the facilities. MAE, SG and WZ edited the manuscript and supported the research. All authors read and approved final manuscript.

**Funding**
This work was supported by National Key R&D Project of China (2022YFE0115400).

**Availability of data and materials**
The data sets used and analyzed during the current study are available from the corresponding author on reasonable request.

## Declarations

**Ethics approval and consent to participate**
This article only has animal subjects performed by the authors. Animal experiments were approved by the Animal Ethics Committee of Shahid Sadoughi University of Medical Sciences and were conducted in accordance with the policies of the Iran National Committee for Ethics in Biomedical Research (IR.SSU.MEDICINE.REC.1400.358).

**Consent for publication**
All authors agree to publish this manuscript in this journal.

**Competing interests**
The author reports no competing interests in this work.

Received: 25 January 2023 Accepted: 6 March 2023
Published online: 19 March 2023

**References**

Abtahi NA, Naghib SM, Haghiralsadat F, Reza JZ, Hakimian F, Yazdian F et al (2021) Smart stimuli-responsive biofunctionalized niosomal nanocarriers for programmed release of bioactive compounds into cancer cells in vitro and in vivo. Nanotechnol Rev 10(1):1895–1911

Abtahi NA, Naghib SM, Ghalekohneh SJ, Mohammadpour Z, Nazari H, Mosavi SM et al (2022) Multifunctional stimuli-responsive niosomal nanoparticles for co-delivery and co-administration of gene and bioactive compound: In vitro and in vivo studies. Chem Eng J 429:132090

Agostini M, Knight RA (2014) miR-34: from bench to bedside. Oncotarget 5(4):872–881

Akhlaghi M, Taebpour M, Lotfabadi NN, Naghib SM, Jalili N, Farahmand L et al (2022) Synthesis and characterization of smart stimuli-responsive herbal drug-encapsulated nanoniosome particles for efficient treatment of breast cancer. Nanotechnol Rev 11(1):1364–1385

Alemi A, Zavar Reza J, Haghiralsadat F, Zarei Jaliani H, Haghi Karamallah M, Hosseini SA et al (2018) Paclitaxel and curcumin coadministration in novel cationic PEGylated niosomal formulations exhibit enhanced synergistic antitumor efficacy. J Nanobiotechnol 16(1):1–20. https://doi.org/10.1186/s12951-018-0351-4

Alhasan L (2019) MiR-126 modulates angiogenesis in breast cancer by targeting. Asian Pacific J Cancer Prevention APJCP 20:193–7

Alkabban FM, Ferguson T. (2018). Cancer, breast.

Alsadat N, Morteza S, Jafari S (2021) Multifunctional stimuli-responsive niosomal nanoparticles for co-delivery and co-administration of gene and bioactive compound: in vitro and in vivo studies. Chem Eng J 2022(429):132090. https://doi.org/10.1016/j.cej.2021.132090

Asthana GS, Sharma PK, Asthana A (2016) In vitro and in vivo evaluation of niosomal formulation for controlled delivery of clarithromycin. Scientifica. https://doi.org/10.1155/2016/6492953

Bader AG, Brown D, Winkler M (2010) The promise of MicroRNA replacement therapymicroRNA replacement therapy. Cancer Res 70(18):7027–30

Bader AG, Brown D, Stoudemire J, Lammers P (2011) Developing therapeutic microRNAs for cancer. Gene Ther 18(12):1121–6

Balakrishnan P, Shanmugam S, Seok W, Mo W, Oh J, Hoon D et al (2009) Formulation and in vitro assessment of minoxidil niosomes for enhanced skin delivery. Int J Pharmaceutics 377:1–8

Barani M, Mirzaei M, Torkzadeh-mahani M (2019) Evaluation of carum-loaded niosomes on breast cancer cells: physicochemical properties, in vitro cytotoxicity, flow cytometric, dna fragmentation and cell migration assay. Sci Rep. https://doi.org/10.1038/s41598-019-43755-w

Barani M, Nematollahi MH, Zaboli M, Mirzaei M, Torkzadeh-Mahani M, Pardakhty A et al (2019) In silico and in vitro study of magnetic niosomes for gene delivery: the effect of ergosterol and cholesterol. Mater Sci Eng 94:234–46. https://doi.org/10.1016/j.msec.2018.09.026

Bartel DP (2004) MicroRNAs: genomics, biogenesis, mechanism, and function. Cell 116(2):281–97

Bartelds R, Nematollahi MH, Pols T, Stuart MCA, Pardakhty A, Asadikaram G et al (2018) Niosomes, an alternative for liposomal delivery. PLoS ONE 13(4):e0194179

Brannon-Peppas L, Blanchette JO (2004) Nanoparticle and targeted systems for cancer therapy. Adv Drug Deliv Rev 56(11):1649–59

Ceren Ertekin Z, Sezgin Bayindir Z, Yuksel N (2015) Stability studies on piroxicam encapsulated niosomes. Curr Drug Deliv 12(2):192–9

Cheok CF (2012) Protecting normal cells from the cytotoxicity of chemotherapy. Cell Cycle 11(12):2227

Davarpanah F, Yazdi AK, Barani M, Mirzaei M (2018) Magnetic delivery of antitumor carboplatin by using PEGylated-Niosomes. DARU J Pharmaceutical Sci. https://doi.org/10.1007/s40199-018-0215-3

Fernandez-Piñeiro I, Badiola I, Sanchez A (2017) Nanocarriers for microRNA delivery in cancer medicine. Biotechnol Adv 35(3):350–60

Francies FZ, Hull R, Khanyile R, Dlamini Z (2020) Breast cancer in low-middle income countries: abnormality in splicing and lack of targeted treatment options. Am J Cancer Res 10(5):1568

Garzon R, Marcucci G, Croce CM (2010) Targeting microRNAs in cancer: rationale, strategies and challenges. Nat Rev Drug Discov 9(10):775–789
Jemal A, Bray F, Center MM, Ferlay J, Ward E, Forman D (2011) Global cancer statistics. CA Cancer J Clin 61(2):69–90
Li XJ, Ren ZJ, Tang JH (2014) MicroRNA-34a: a potential therapeutic target in human cancer. Cell Death Dis 5(7):e1327–e1327
Lin Y-L, Liu Y-K, Tsai N-M, Hsieh J-H, Chen C-H, Lin C-M et al (2012) A Lipo-PEG-PEI complex for encapsulating curcumin that enhances its antitumor effects on curcumin-sensitive and curcumin-resistance cells. Nanomed Nanotechnol Biol Med 8(3):318–27
Lv S, Tang Z, Li M, Lin J, Song W, Liu H et al (2014) Co-delivery of doxorubicin and paclitaxel by PEG-polypeptide nanovehicle for the treatment of non-small cell lung cancer. Biomaterials 35(23):6118–29. https://doi.org/10.1016/j.biomaterials.2014.04.034
Matsumura Y, Maeda H (1986) A new concept for macromolecular therapeutics in cancer chemotherapy: mechanism of tumoritropic accumulation of proteins and the antitumor agent smancs. Cancer Res 46(1):6387–92
Mazidi Z, Javanmardi S, Naghib SM, Mohammadpour Z (2022) Smart stimuli-responsive implantable drug delivery systems for programmed and on-demand cancer treatment: An overview on the emerging materials. Chem Eng J 433:134569
Momenimovahed Z, Salehiniya H (2019) Epidemiological characteristics of and risk factors for breast cancer in the world. Breast Cancer Targets Ther. https://doi.org/10.2147/BCTT.S176070
Navarro F, Lieberman J (2015) miR-34 and p53: New Insights into a Complex Functional Relationship. PLoS ONE 10(7):e0132767
Okada N, Lin C-P, Ribeiro MC, Biton A, Lai G, He X et al (2014) A positive feedback between p53 and miR-34 miRNAs mediates tumor suppression. Genes Dev 28(5):438–50
Rahimzadeh Z, Naghib SM, Askari E, Molaabasi F, Sadr A, Zare Y et al (2021) A rapid nanobiosensing platform based on herceptin-conjugated graphene for ultrasensitive detection of circulating tumor cells in early breast cancer. Nanotechnol Rev 10(1):744–753
Rahmani AH, Almatroudi A, Babiker AY, Khan AA, Alsahli MA (2019) Thymoquinone, an active constituent of black seed attenuates CCl4 induced liver injury in mice via modulation of antioxidant enzymes, PTEN, P53 and VEGF protein. Open access Maced J Med Sci 7(3):311
Sadeghi M, Kashanian S, Naghib SM, Arkan E (2022) A high-performance electrochemical aptasensor based on graphene-decorated rhodium nanoparticles to detect HER2-ECD oncomarker in liquid biopsy. Sci Rep 12(1):1–12
Sadeghi M, Kashanian S, Naghib SM, Askari E, Haghiralsadat F, Tofighi D (2022) A highly sensitive nanobiosensor based on aptamer-conjugated graphene-decorated rhodium nanoparticles for detection of HER2-positive circulating tumor cells. Nanotechnol Rev 11(1):793–810
Schoof CRG, da Silva Botelho EL, Izzotti A, dos Reis VL (2012) MicroRNAs in cancer treatment and prognosis. Am J Cancer Res 2(4):414
Siddiqui AA, Amin J, Alshammary F, Afroze E, Shaikh S, Rathore HA et al (2021) Burden of cancer in the Arab world. Handb Healthc Arab world. https://doi.org/10.1007/978-3-030-36811-1_182
Smaili F, Boudjella A, Dib A, Braikia S, Zidane H, Reggad R et al (2020) Epidemiology of breast cancer in women based on diagnosis data from oncologists and senologists in Algeria. Cancer Treat Res Commun 25:100220
Wang Y, Yu J, Cui R, Lin J, Ding X (2016) Curcumin in treating breast cancer: a review. J Laboratory Automation. https://doi.org/10.1177/2211068216655524
Yaghoubi F, Naghib SM, Motlagh NSH, Haghiralsadat F, Jaliani HZ, Tofighi D et al (2021) Multiresponsive carboxylated graphene oxide-grafted aptamer as a multifunctional nanocarrier for targeted delivery of chemotherapeutics and bioactive compounds in cancer therapy. Nanotechnol Rev 10(1):1838–1852

## Publisher's Note